Monthly variability in surface pCO_2 and net air-sea CO_2 flux in the Arabian Sea

V. V. S. S. Sarma[1]

Centre Européen de Recherche et d'Enseignement de Géosciences de l'Environnement, Europole de l'Arbois, Aix en Provence, France

Received 17 July 2001; revised 17 April 2003; accepted 8 May 2003; published 12 August 2003.

[1] Recent studies on biogeochemical cycling of carbon in the Arabian Sea, by Joint Global Ocean Flux Study (JGOFS), revealed that the Arabian Sea is a perennial source of carbon dioxide to the atmosphere. The surface pCO_2 is governed by physical processes such as water mass transports, upwelling and winter convective mixing, and associated biological processes. Hence surface pCO_2 distribution showed significant seasonal and spatial variability. As a result, it is difficult to extrapolate observed data to the entire basin to assess basin-wide fluxes of CO_2 to the atmosphere. On the basis of the data collected during Indian, U.S. JGOFS, and Indian Land-Ocean Interactions in the Coastal Zone process study programs in the Arabian Sea, multiple regression equations were developed on a seasonal basis to compute dissolved inorganic carbon (DIC) from surface temperature, salinity, and chlorophyll as constraints. Total alkalinity (TA) was computed from surface salinity. On the basis of satellite derived chlorophyll (Coastal Zone Color Scanner) and Levitus surface temperature and salinity climatology, surface TA and DIC were constructed at $1^\circ \times 1^\circ$ grids. Using carbonate dissociation constants, pCO_2 levels were computed. The results show the southwest coast of India occupied with very low-pCO_2 waters because of inflow from Bay of Bengal low-saline water mass during NE monsoon (December–February). On the other hand, this area is occupied with pCO_2-rich (>500 μatm) waters during SW monsoon (June–August) because of coastal upwelling. The highest pCO_2 (>700 μatm) were found along the west coast of the Arabian Sea driven by strong upwelling. In the open ocean, higher pCO_2 levels were observed in the north (north of 15°N) compared to the southern Arabian Sea round the year, with values higher than those in the atmosphere even in the south. Though no strong physical forcing occurs during spring intermonsoon (March–May), surface pCO_2 levels were higher than in the atmosphere. The air-sea flux of CO_2 was found to be high during SW monsoon throughout the Arabian Sea. The west coast of the Arabian Sea releases higher quantities of CO_2 to the atmosphere per unit area followed by the northern and eastern Arabian Sea. As a whole, the Arabian Sea (north of 10°N) releases about 90 TgC yr^{-1} to the atmosphere. *INDEX TERMS:* 4227 Oceanography: General: Diurnal, seasonal, and annual cycles; 4805 Oceanography: Biological and Chemical: Biogeochemical cycles (1615); 4806 Oceanography: Biological and Chemical: Carbon cycling; *KEYWORDS:* carbon dioxide, air-sea exchange, seasonal cycles, budgets, Arabian Sea

Citation: Sarma, V. V. S. S., Monthly variability in surface pCO_2 and net air-sea CO_2 flux in the Arabian Sea, *J. Geophys. Res.*, *108*(C8), 3255, doi:10.1029/2001JC001062, 2003.

1. Introduction

[2] Measurements of atmospheric CO_2 imply that oceans and terrestrial biosphere absorb about half of the anthropogenic CO_2 emissions each year, but the quantitative differentiation of the oceanic and biospheric carbon sinks remain unclear [*Siegenthaler and Sarmiento*, 1993]. The estimation of air-sea fluxes of carbon dioxide requires knowledge of the large-scale spatiotemporal distribution of carbon dioxide partial pressures (pCO_2), which is difficult to obtain from observations only. Recently, *Takahashi et al.* [2002] mapped air-sea fluxes of CO_2 for the World Oceans, on the basis of the available data, and suggested that Arabian Sea is acting as a source for atmospheric carbon dioxide except a small region in the south west coast of India. These fluxes are close to the fluxes observed at equatorial region in the Pacific Ocean. Recent observations by Joint Global Ocean Flux Study (JGOFS) in the Arabian Sea revealed that this region is acting as a perennial source of carbon dioxide to the atmosphere with large seasonal variability [*Sarma et al.*, 1996, 1998; *Körtzinger et al.*, 1997; *Goyet et al.*, 1998a; *Sarma*, 1998].

[1]Now at Hydrospheric-Atmospheric Research Center, Nagoya University, Nagoya, Japan.

0148-0227/03/2001JC001062

[3] Seasonal variability in physical associated biogeochemical cycling of carbon and nitrogen [*de Sousa et al.*, 1996; *Prasanna Kumar and Prasad*, 1996, *Madhupratap et al.*, 1996; *Morrison et al.*, 1998; *Sarma*, 1998] and variability in surface dissolved inorganic carbon (DIC) and pCO_2 have been discussed in detail elsewhere [*Millero et al.*, 1998; *Goyet et al.*, 1998a; *Sarma et al.*, 1996, 1998; *Körtzinger et al.*, 1997; *Sarma*, 1998; *Sarma et al.*, 2000]. On the basis of different physical and meteorological processes, the study region can be classified as four seasons. They are northeast (NE) (December–February), spring inter- (March–May), southwest (SW) (June–August), and fall monsoons (September–November). During NE monsoon, low SSTs (24°–25°C) are obvious in the northern Arabian Sea because of winter convective mixing driven by NE trade winds [*Madhupratap et al.*, 1996]. This leads to pumping of waters enriched in subsurface DIC and pCO_2 into the surface. Surface currents in the open sea are equator ward whereas it is opposite in the east coast of the Arabian Sea. A branch of NE monsoon currents turns north and flows along the west coast of India during December–January, bringing low-salinity surface waters from the Bay of Bengal [*Shetye and Shenoi*, 1988]. On the other hand, SST rises up to 29°–31°C during spring intermonsoon with low north-south gradient [*Prasanna Kumar and Prasad*, 1996]. Strong stratification with shallow mixed layer depth is obvious during this season. Intense coastal upwelling is noticed along the Somalia and Arabia coasts in the west coast of the Arabian Sea [*Wyrtki*, 1973; *Morrison et al.*, 1998] while mild upwelling was observed in the SW coast of India during SW monsoon [*Shetye et al.*, 1990; *Muralidheeran and Prasanna Kumar*, 1996]. As a result of these physical processes, biological activity is enhanced by several folds. For instance, Chlorophyll concentrations ranged between 0.064–0.27 mg m^{-3} during NE monsoon, 0.02–0.2 mg m^{-3} during intermonsoon and 0.32–1.2 mg m^{-3} during SW monsoon seasons respectively [*Bhattathiri et al.*, 1996; *Barber et al.*, 2001]. Bacterial respiration in the surface layer was found to be higher during intermonsoon seasons and was attributed to time lag between phytoplankton production and bacterial response [*Ramaiah et al.*, 1996]. High pCO_2 levels during intermonsoon were attributed to high bacterial respiration in the mixed layers [*Sarma et al.*, 2000].

[4] Basically these field measurements of pCO_2 reveal high temporal and spatial variations in surface pCO_2 distribution in the Arabian Sea. These variations are linked to dynamical and biogeochemical processes which are not well quantified and therefore making flux estimates on basin scale is difficult. *Goyet et al.* [1998a] computed surface pCO_2 on the basis of observed relation between underway surface pCO_2 and sea surface temperature and suggested that 7 TgC yr^{-1} is released annually to the atmosphere from the Arabian Sea. On the basis of Indian JGOFS data, *Sarma et al.* [1998] computed the emission of CO_2 to the atmosphere by the central and eastern Arabian Sea to be 45 TgC yr^{-1}. Recently *Sabine et al.* [2000] estimated fluxes of pCO_2 to the atmosphere by the entire Indian Ocean on the basis of U.S. JGOFS and WOCE data using a multiparameter fit. They estimated that Arabian Sea (north of equator) releases >150 TgC yr^{-1} (>2 mole CO_2 m^{-2} yr^{-1}) to the atmosphere. *Goyet et al.* [1998a] flux estimate seems to be underestimated as the surface pCO_2 is constructed using relation between temperature and underway pCO_2 that showed large scatter. They attributed that the uncertainties in the surface pCO_2 levels, especially in the coastal regions where pCO_2 changes are large, are due to biological activity which is explicitly did not taken into account. On the other hand, the estimate by *Sarma et al.* [1998] is based on extrapolation of computed pCO_2 data along cruise tracks to the eastern and central Arabian Sea, which may not always be reliable. *Louanchi et al.* [1996] evaluated different effects, such as biology, mixing, thermodynamics and fluxes, on surface pCO_2 in the Indian Ocean. However, regenerated carbon in the mixed layer was considered to be 50% of photosynthetically produced carbon during all seasons in their model, which seems to be too low on the basis of recent JGOFS estimates [e.g., *Ramaiah et al.*, 1996]. *Goyet et al.* [1998b] modified this model by considering euphotic zone chlorophyll concentration instead of mixed layer chlorophyll and considered 50% of the photosynthetically produced carbon is regenerated in the surface layers. However, they have not made any flux estimate for the Arabian Sea.

[5] Recently, *Lee et al.* [2000] computed surface DIC concentrations on the basis of relationships of DIC with temperature and nitrate using WOCE data set but no seasonal variability is considered. Moreover, they did not use any data in the Arabian Sea, north of 10°N, in the regression analysis. Nevertheless, the data show (plates 2 and 3) very weak north south gradients in DIC distribution in the Arabian Sea. This study suggests that seasonal regression fits would help to understand spatial variability in DIC driven by different physical and biogeochemical processes. The idea underlying in this study is to use variations in satellite derived chlorophyll and climatological fields to constrain the spatiotemporal distribution of pCO_2 and to obtain large-scale regional distribution of pCO_2 and its fluxes to the atmosphere.

2. Material and Methods

[6] Data used in this study were collected during different seasons and the sources were listed in Table 1. The tracks of different cruises are plotted in Figure 1. Temperature and salinity data were collected using a Seabird CTD system. Total alkalinity (TA) was measured potentiometrically in U.S. JGOFS cruises [see *Millero et al.*, 1998]. Total carbon dioxide (DIC) was measured by coulometric technique using semiautomated subsampling system during Indian JGOFS and Land-Ocean Interactions in the Coastal Zone (LOICZ) programs [*Sarma et al.*, 1996, 1998; *Sarma*, 1998] whereas it was done using WHOI Dissolved Inorganic Carbon Extractor (DICE) coulometry system [*Millero et al.*, 1998] under U.S. JGOFS process study. DIC measurements were regularly checked against sodium carbonate standards and necessary corrections were applied to the data sets. In addition to this, measurements of TA and DIC of the Certified Reference Materials (CRM, batch 28 for Indian JGOFS and LOICZ, and 22, 26, 28, 29 and 30 for U.S. JGOFS, supplied by A. Dickson, Scripps Institution of Oceanography, La Jolla, California) revealed accuracies within ±2.0 μmol Kg^{-1} for DIC during Indian JGOFS and LOICZ cruises, and ±0.7 and ±2 μmol kg^{-1} for DIC

Table 1. Details of Indian, U.S. JGOFS, and LOICZ Cruises, the Data of Which Were Used in This Study

Study Program	Area	Ship	Cruise Number	Cruise Dates
U.S. JGOFS	Western and central Arabian Sea	*Thompson*	TTN 043	8 Jan. 1995 to 5 Feb. 1995
U.S. JGOFS	Western and central Arabian Sea	*Thompson*	TTN 045	4 March 1995 to 10 April 1995
U.S. JGOFS	Western and central Arabian Sea	*Thompson*	TTN 049	17 July 1995 to 15 Aug. 1995
U.S. JGOFS	Western and central Arabian Sea	*Thompson*	TTN 054	30 Nov. 1995 to 28 Dec. 1995
Indian JGOFS	Eastern and central Arabian Sea	*Sagar Kanya*	SK 91	13 April 1994 to 11 May 1994
Indian JGOFS	Eastern and central Arabian Sea	*Sagar Kanya*	SK99	3 Feb. 1995 to 3 March 1995
Indian JGOFS	Eastern and central Arabian Sea	*Sagar Kanya*	SK104	20 July 1995 to 12/Aug. 1995
Indian JGOFS	Eastern and central Arabian Sea	*Sagar Kanya*	SK115	4–20 Aug. 1996
Indian JGOFS	Eastern and central Arabian Sea	*Sagar Kanya*	SK121	4–25 Feb. 1997
LOICZ	Eastern and central Arabian Sea	*Sagar Kanya*	SK103	26 June 1995 to 5 July 1995
LOICZ	Eastern and central Arabian Sea	*Sagar Sampada*	SS 136	8–20 Sept. 1995
LOICZ	Eastern and central Arabian Sea	*Sagar Sampada*	SS141	25 April 1996 to 14 May 1996

and TA, respectively, for U.S. JGOFS process study cruises. The data collected within the frame work of U.S. JGOFS are available at http://usjgofs.whoi.edu/ and Indian JGOFS data can be obtained from http://www.indian-ocean.org/support/main.html.

3. Model Description

[7] In order to assess surface pCO_2 variability at high resolution in the Arabian Sea, a multiparameter fit method was used here. The mixed layer DIC showed distinct relationships with respect to temperature, salinity, and chlorophyll (Figures 2a–2c). The slope and intercepts of these relations, however, have shown strong seasonal variability. DIC showed negative relation with temperature, in general, but with seasonal changes in slopes. On the contrary, salinity showed positive relation with DIC in all the seasons except during SW monsoon when it showed negative that can be attributed to coastal and open ocean upwelling driven by winds and Findlater jet, respectively [*Findlater*, 1969, 1974; *Shetye et al.*, 1990; *Muralidheeran et al.*, 1996]. In contrast, chlorophyll exhibited weak positive relation with DIC in all the seasons except fall monsoon. Despite low chlorophyll levels, DIC concentration increases because of decomposition of organic matter that resulted in negative relation during fall monsoon. As a whole, the weak relationship between DIC and chlorophyll during all seasons could be due to dominant effect of mixing on DIC levels [*Sarma et al.*, 2000]. Moreover, no strong relations can be expected for DIC either with temperature, salinity or chlorophyll because all these parameters influence DIC content in different directions and magnitudes. Earlier investigators used either temperature [*Goyet et al.*, 1998a] or temperature and salinity [*Sabine et al.*, 2000] as a constraint to extrapolate surface pCO_2, but *Takahashi et al.* [2002] reveal that biology is very important on draw down of pCO_2 in the Arabian Sea that amounts to ~40–170 μatm which is more than temperature effect (~40–80 μatm). Hence chlorophyll was considered as a constraint in the present study to construct surface DIC on basin scale. Multiple regression equations were developed for different seasons using the mixed layer temperature, salinity and chlorophyll. The resultant regression fits are:

NE monsoon

$$\mathrm{DIC} = 845.74 - 20.88\ \mathrm{T} + 47.79\ \mathrm{S} - 34.37\mathrm{Chl}\left[\pm 5\ \mu\mathrm{mol\,kg^{-1}}\right] \quad (1)$$

Spring monsoon

$$\mathrm{DIC} = 1071.58 - 17.471\ \mathrm{T} + 39.23\ \mathrm{S} - 31.478\mathrm{Chl}\left[\pm 6.5\mu\mathrm{mol\,kg^{-1}}\right] \quad (2)$$

SW monsoon

$$\mathrm{DIC} = 1454.4 - 23.1\ \mathrm{T} + 33.37\ \mathrm{S} - 23.82\mathrm{Chl}\left[\pm 6\mu\mathrm{mol\,kg^{-1}}\right] \quad (3)$$

Fall monsoon

$$\mathrm{DIC} = 865.5 - 7.6\ \mathrm{T} + 37.8\ \mathrm{S} - 37.9\mathrm{Chl}\left[\pm 8\mu\mathrm{mol\,kg^{-1}}\right] \quad (4)$$

[8] Here T is temperature (°C), S is salinity and Chl is chlorophyll in mg m^{-3}. The results of sensitivity test of the parameters used in the above equations are given in Table 2. These results show that the influence of temperature is higher during monsoons compared to nonmonsoon seasons. This is consistent with *Sarma et al.* [2000], who suggest mixing is the main controlling factor on surface DIC concentrations during monsoons. The effect of change in unit of salinity is comparatively higher during NE monsoon (47.78 μmol kg^{-1}) and it is more or less constant (~35 μmol kg^{-1}) during other seasons. The higher influ-

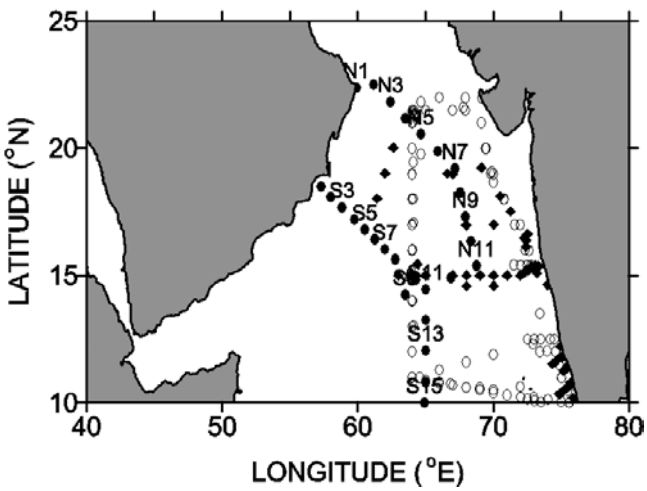

Figure 1. Cruise tracks that show the data collected during Indian (open circles), U.S. JGOFS Process study (solid circles), and LOICZ programs (solid diamonds).

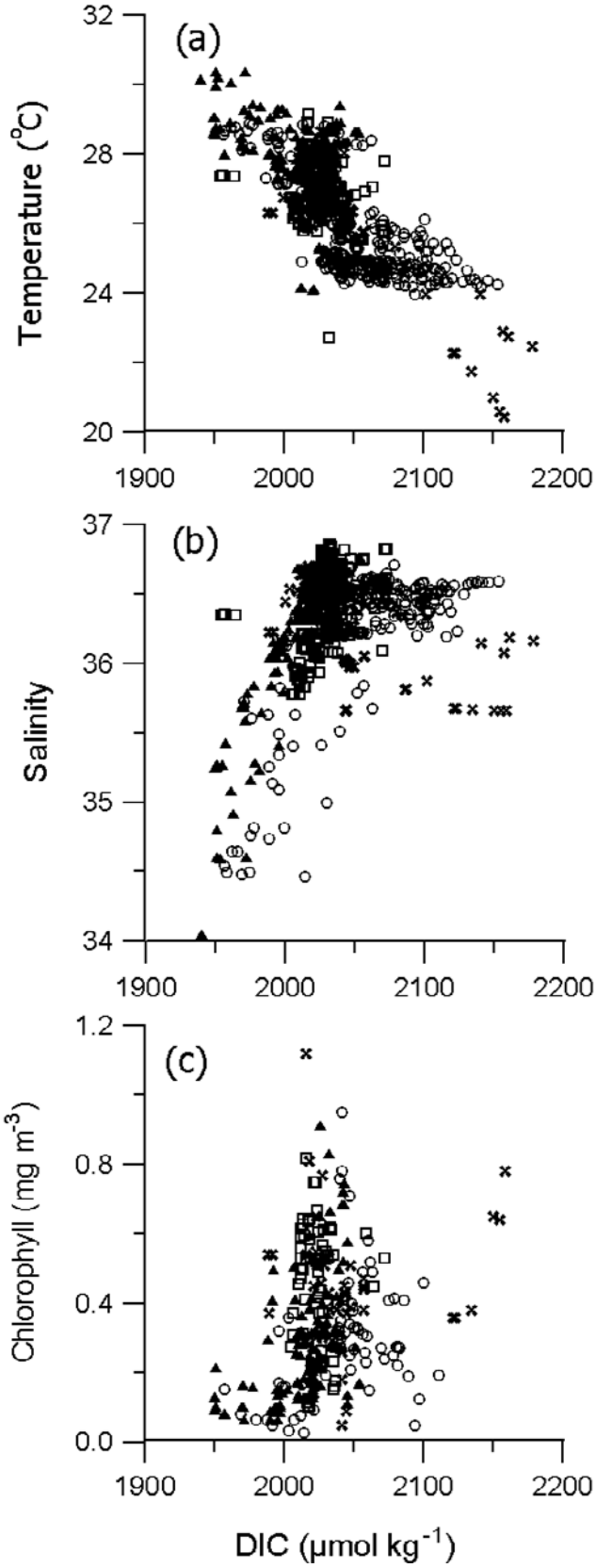

Figure 2. Relationship of DIC with (a) temperature, (b) salinity, and (c) chlorophyll for the data used for developing multiple regression equations. NE monsoon (open circle), spring intermonsoon (triangle), SW monsoon (cross), and fall intermonsoon (open square).

Table 2. Results of Sensitivity Test of the Multiple Regression Equations

Months	Parameter	Change in DIC μmol per Unit Increase in Parameter
Dec., Jan., and Feb.	temperature	−20.8
	salinity	+47.8
	chlorophyll	−34.4
March, April, and May	temperature	−17.0
	salinity	+39.2
	chlorophyll	−37.5
June, July, and Aug.	temperature	−23.1
	salinity	+33.4
	chlorophyll	−23.8
Sept., Oct., and Nov.	temperature	−7.6
	salinity	+37.8
	chlorophyll	−37.9

ence of salinity during NE monsoon is due to high evaporation leads to formation of Arabian Sea high-saline water mass (ASH) in the northern Arabian Sea result to increase in DIC concentrations. The effect of change in 1 mg m^{-3} chlorophyll is more or less constant during all seasons except SW monsoon. This could be due to less seasonal variability in column production in the Arabian Sea [*Barber et al.*, 2001].

[9] On the other hand, TA showed strong correlation with salinity. Hence TA is computed from the surface salinity using the following equation:

$$\mathrm{TA} = 350.8 + 55.6\ \mathrm{S}\left(\pm 5.7\ \mu\mathrm{mol\,kg^{-1}}\right) \qquad (5)$$

This equation was determined using the geometric mean of the data from U.S. JGOFS cruises in the Arabian Sea and the data from the WOCE cruises II across the Arabian Sea and the Bay of Bengal [*Goyet et al.*, 1999]. This equation is valid for the salinity range of 31 to 36.8. *Goyet et al.* [1999] have found that surface TA maxima and minima are coincided with salinity maxima and minima.

[10] The pCO_2 is computed from DIC, TA, and Levitus nutrient climatology [*Conkright et al.*, 1988] using the CO_2SYS program [*Lewis and Wallace*, 1998] and carbonate dissociation constants of *Mehrbach et al.* [1973], that were refit by *Dickson and Millero* [1987], at in situ temperature and salinity. These constants were found to be the best to compute pCO_2 from DIC and TA couple [*Wanninkhof et al.*, 1999; *Johnson et al.*, 1999]. However, I have compared pCO_2 computed with these constants to that of *Goyet and Poisson* [1989] and found that pCO_2 computed using dissociation constants of *Goyet and Poisson* are higher by 16–20 μatm to that of *Mehrbach* constants and the difference also seems to be very systematic. The difference, however, is more (∼20 μatm) during June–August than in other months (16–18 μatm). Moreover, pCO_2 computed from DIC and TA couple using *Mehrbach et al*., constants is comparable with underway pCO_2 of *Goyet et al.* [1998a] within the ±6–7 μatm.

[11] On the basis of existence of different biogeochemical provinces, the study region is divided into three part, they are the west coast of the Arabian Sea (WAS), the east coast of the Arabian Sea (EAS) and the open sea region of northern Arabian Sea (NAS). Among these regions, intense upwelling takes place in the WAS and mild to moderate upwelling in the EAS during SW monsoon, winter convec-

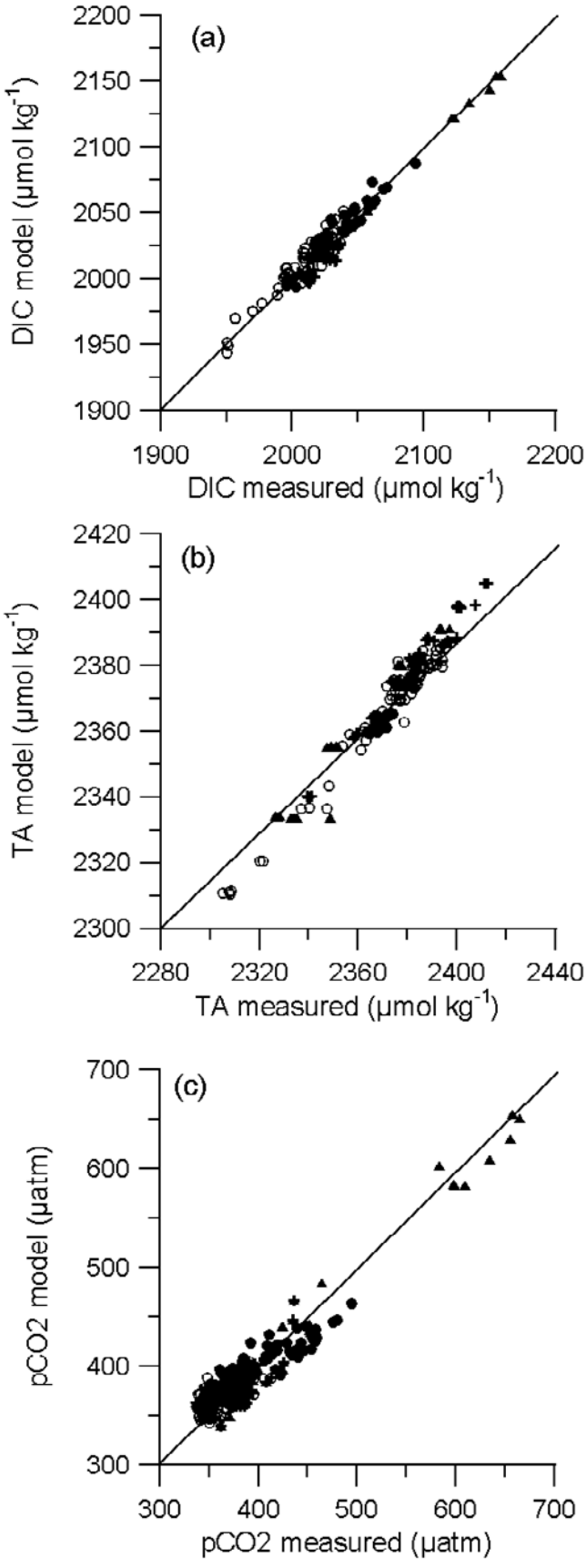

tive mixing and open ocean upwelling takes place in the NAS during NE and SW monsoons respectively. EAS and WAS is separated on the basis of 200 m bottom topography. Because of the lack of data in the south of 10°N, the budget construction was restricted to the north of 10°N for the Arabian Sea.

4. Constraints

[12] The constraints of this model are monthly means of surface temperature, salinity, Coastal Zone Color Scanner chlorophyll and wind speeds at $1° \times 1°$ grid levels. Here I used climatological data [*Levitus and Boyer*, 1994; *Levitus et al.*, 1994] for surface temperature and surface salinity whereas wind speed was obtained from *Hellerman and Rosenstein* [1983]. The errors in the computation of pCO_2 from DIC and TA couple varied from ±18 to 23 µatm. This includes the errors associated with the temperature, salinity, and chlorophyll. In order to verify this model, several U.S., Indian JGOFS, and LOICZ stations data of TA and DIC and computed pCO_2 from them and also underway pCO_2 during different seasons have been compared with modeled results in Figure 3a–3c. This shows that the modeled surface TA, DIC and pCO_2 concentrations reproduce the observed concentrations reasonably well. The errors involved in the reproduction of observed pCO_2 levels were found to be within ±5–30 µatm. The deviations are mostly found in the coastal regions. However, most of these differences in pCO_2 are within the uncertainties involved in pCO_2 computations.

5. Results and Discussion

5.1. Variability in Surface DIC

[13] The seasonal variability in surface DIC for January, April, July, and October are presented in Figures 4a–4d. DIC showed strong spatial variability during all the seasons. During January, SW coast of India exhibited very low concentrations of DIC (1940–1960 µmol kg^{-1}) that can be attributed to the occurrence of Bay of Bengal low-saline water mass [*Shetye and Shenoi*, 1988], which contains low DIC [*Kumar et al.*, 1996]. Bay of Bengal receives enormous amount of river water from the Ganges, Brahmaputra and Irrawaddy-Salween system with low DIC concentrations [*Shetye and Shenoi*, 1988]. This result in strong E-W gradient in DIC by ~40 µmol kg^{-1} could be due to occurrence of low-salinity waters in the east. DIC concentrations are higher in the north and western Arabian Sea than in other areas during January. Higher DIC concentrations (2020–2030 µmol kg^{-1}) in the north can be attributed to winter convective mixing [*Sarma et al.*, 1996, 1998].

Figure 3. (opposite) Relation between different measured inorganic carbon parameters in different seasons to modeled data (a) DIC, (b) TA, and (c) pCO_2. NE monsoon (solid circle), spring intermonsoon (open circle), SW monsoon (triangle), and fall monsoon (plus). The pCO_2 measured denotes both pCO_2 computed from measured DIC and TA and underway pCO_2. The 1:1 line has been drawn to show their agreement.

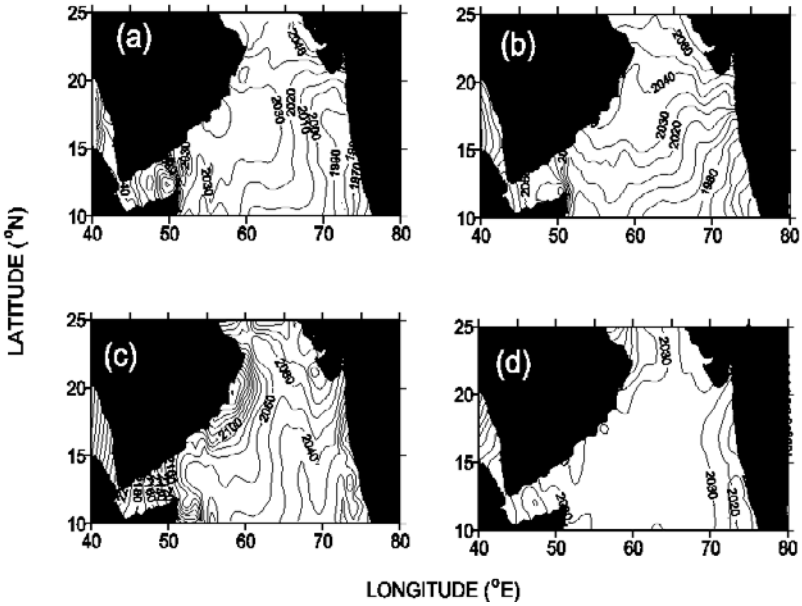

Figure 4. Distribution of DIC during different months in the Arabian Sea: (a) January, (b) April, (c) July, and (d) October. Note the contour interval for Figure 4c is changed to 20 for contours above 2050 μmol.

[14] The gradient between north and south is as large as 60 μmol kg^{-1} during April, however, the east west gradient is very small (~10 μmol kg^{-1}; Figure 4b). DIC concentrations along SW coast of India are lower than in January (<1940 μmol kg^{-1}). The low concentrations of DIC in the south can be attributed to the influence of southern Indian Ocean waters as the circulation pattern reverses during spring intermonsoon from equatorward flow to poleward [*Shetye and Shenoi*, 1988]. On the other hand, DIC concentrations are high in all regions during July that ranged from 1980 to 2145 μmol kg^{-1} (Figure 4c). The DIC concentrations are especially very high along west coast of the Arabian Sea (2150 μmol kg^{-1}) because of occurrence of intense upwelling along this coast [*Wyrtki*, 1973; *Morrison et al.*, 1998]. This result in strong east-west gradient (~120 μmol kg^{-1}) develops during July in the Arabian Sea. On the other hand, DIC concentrations are more or less uniform (~2025 μmol kg^{-1}) during October throughout the Arabian Sea with less north south and east-west gradients (Figure 4d).

5.2. Monthly and Spatial Variability in Surface pCO_2

[15] Surface water pCO_2 levels are controlled by an intricate interplay of biological, chemical and physical processes in seawater [*Takahashi et al.*, 1993]. The monthly variability in surface pCO_2 distribution at three selected locations suggests that it followed monsoonal cycle. A pCO_2 minimum occurred in April/May and September/October whereas maximum found during July/August (Figures 5a–5c) and this pattern is well represented the observed behavior [*Sarma et al.*, 1996, 1998]. The amplitude of seasonal variations in pCO_2 in surface seawater is approximately 10 to 40 μatm in the Arabian Sea with strong spatial variability. Rapid changes in surface pCO_2 from May

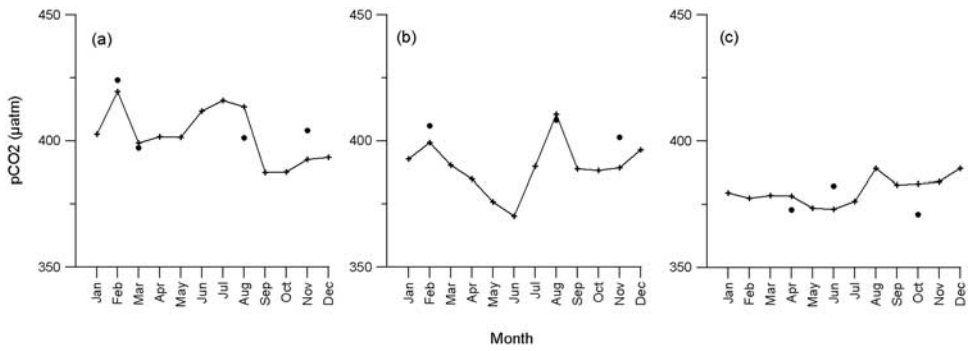

Figure 5. Monthly variability in surface pCO_2 at different locations in the Arabian Sea: (a) 9°N, 67°E, (b) 14°N, 65°E, and (c) 15°N, 70°E. Solid circles denote pCO_2 computed from measured DIC and TA, and solid lines with pluses represent modeled pCO_2.

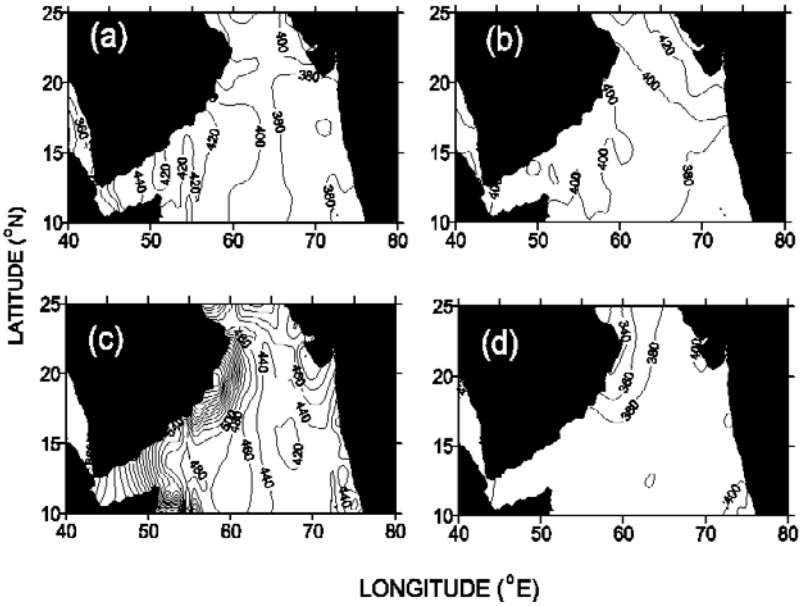

Figure 6. Monthly and spatial variability in surface pCO_2 distribution in the Arabian Sea: (a) December–February, (b) March–May, (c) June–August, and (d) September–October. Note the contour interval for Figure 4c is changed to 40 for contours above 500 μatm.

to June and August to September are resulted by changes in temperature followed by chlorophyll. For clarity of presentation to examine spatial variability in surface pCO_2 distribution, monthly pCO_2 levels are averaged to represent four seasons and discussed in the following sections.

5.2.1. December, January, and February (NE Monsoon)

[16] As explained in the section 5, convective mixing takes place in the northern Arabian Sea (north of 15°N) during NE monsoon. The pCO_2 levels in the central Arabian Sea range from 380 to 420 μatm during NE monsoon (Figure 6a). The east-west gradient of pCO_2 is as high as 40 μatm with lower values in the east because of Bay of Bengal low-salinity water mass. As a result of this water mass, low pCO_2 (<360 μatm) levels observed between east of 72°E and south of 13°N along the southwest coast of India during NE monsoon. When this mass flows toward north, they mix up with the local high-pCO_2 waters and their signature vanishes toward north. On contrary, this region is occupied with relatively high pCO_2 levels of 370–380 μatm during spring intermonsoon (Figures 6b–6d). This feature is consistent with the CO_2 flux estimated by *Takahashi et al.* [2002] that showed SW coast of India is a sink for atmospheric CO_2 and also agrees with the observations of *Sarma et al.* [1998].

5.2.2. March, April, and May (Spring Intermonsoon)

[17] These months represent transition period between NE to SW monsoon when winds reverse their direction. During this period, high sea surface temperatures (29°–31°C) are observed because of high solar radiation [*Prasanna Kumar and Prasad*, 1996; *Madhupratap et al.*, 1996]. Shallow mixed layer depths (10–30 m) are obvious during this season because of strong stratification.

[18] The pCO_2 levels during this season in the northern Arabian Sea are higher than in the south by ~20 μatm (Figure 6b). Surface pCO_2 levels are slightly higher than in the NE monsoon. This could be due to increased surface temperature from March to May result in decrease in solubility of CO_2. This suggests that high pCO_2 levels were predominantly result from a thermodynamic response. The surface circulation pattern changes from equator to poleward and hence movement of low-pCO_2 waters toward north can be seen during this season (Figure 6b). Northeastern Arabian Sea showed comparatively high pCO_2 levels (>420 μatm), which could be due to bacterial regeneration of organic matter that has been produced during NE monsoon. *Shetye et al.* [1992] observed the coldest waters in the NE Arabian Sea during NE monsoon compared to other regions in the northern Arabian Sea and suggested that convective mixing is more intense in this region. Moreover, high bacterial activity was observed during intermonsoon and attributed to time lag between organic matter production in the NE monsoon to bacterial response [*Ramaiah et al.*, 1996]. The levels of pCO_2 in the coastal regions have been increased from <360 μatm during NE monsoon to 370–380 μatm during these months because of reversing surface circulation pattern along this coast and hence reduced influence of Bay of Bengal low-salinity water mass. The strong east-west gradient of ~40 μatm during NE monsoon has been decreased to ~20 μatm during spring intermonsoon (Figure 6b). This gradient becomes stronger in the later season as discussed in the following section.

5.2.3. June, July, and August (SW Monsoon)

[19] The flow pattern seen during this season is just opposite to that found during NE monsoon. This reversal actually starts in February and completes by May. The westbound NE monsoon current is replaced by an eastbound monsoon current. During these months, the overall direction of winds over the north Indian Ocean is generally from the southwest and surface current flows toward poleward whereas in the coastal regions it is in the opposite direction. The occurrence of upwelling is the

Table 3. The pCO_2 Levels in the Atmosphere During 1995[a]

Month	pCO_2^{air}, μatm
Jan.–Feb.	353–356
March–May	348–351
June–Sept.	338–342
Oct.–Nov.	335–341
Dec.	336–354

[a]After *Goyet et al.* [1998a].

major characteristic of southwest monsoon season in the Arabian Sea.

[20] The highest pCO_2 levels occurred in surface waters during this season compared to other seasons. During this time, pCO_2 levels are higher than 420 μatm in the central Arabian Sea (Figure 6c). As high as ~700 μatm of surface pCO_2 has been observed in the western upwelling region whereas >480 μatm were noticed along the SW coast of India. These observations are consistence with the observed pattern [*Körtzinger et al.*, 1997; *Goyet et al.*, 1998a; *Sarma et al.*, 1996, 1998]. Strong coastal to offshore gradients are developed in the Arabian Sea because of the occurrence of strong coastal upwelling. *Manghnani et al.* [1998] observed advection of upwelled waters in to the central Arabian Sea during SW monsoon. The simulated pCO_2 levels are consistence with the observed pattern that upwelled high-pCO_2 waters seems to be advected up to east of ~62°E (Figure 6c). *Sarma et al.* [1996] observed high pCO_2 (>420 μatm) in the central Arabian Sea (along 64°E and north of 15°N) during SW monsoon and attributed to open ocean upwelling driven by Findlater jet. However, this feature is not prominent in the simulated pCO_2 distribution (Figure 6c) could be due to masking of this feature by advected high-pCO_2 upwelled waters from the west coast of the Arabian Sea. Along the SW coast of India, the gradient between north and south is small (<20 μatm) whereas east-west gradient is very strong (~300 μatm) during SW monsoon because of different upwelling intensities along east and west coasts. *Shetye et al.* [1990] suggested that upwelling is more intense along the SW coast of India and appeared to become weak north of 15°N. Very high pCO_2 (about 680 μatm) levels were observed along the SW coast of India, south of 8°N, and low-saline waters in the form of continental discharge hinders upwelled water to reach to the surface [*Narvekar et al.*, 1996; *Sarma*, 1998]. *Sarma* [1998] observed patchy distribution with very high and low pCO_2 levels along the east coast because of low dense water capping on upwelled waters. In the simulated pCO_2, this feature is not well depicted because of the use of averaged salinity; nevertheless, upwelling feature is well evident.

5.2.4. September, October, and November (Fall Monsoon)

[21] The conditions in these three months are similar to that found during March–May. This is again the transition period between SW to NE monsoons. During these months, winds change their direction from SW to NE and surface circulation from poleward to equatorward in the central Arabian Sea. Sea surface temperature increases by 2°–3°C compared to August because of increased solar radiation and shallow mixed layer depth.

[22] The surface pCO_2 levels have been found to decrease from >600 μatm to 360–380 μatm off Arabia coast (Figure 6d). This could be attributed to removal by biological processes and also to strong stratification. Consistently high chlorophyll concentrations observed during September because of the availability of nutrients driven by upwelling in the previous months. On the other hand, pCO_2 levels in the central Arabian Sea are ranged between 370 to 380 μatm because of increased surface water temperatures as a result of increased solar radiation. In addition to this, increased bacterial respiration [*Ramaiah et al.*, 1996], enhances the rate of decomposition of organic matter that was produced in the earlier season result in high pCO_2 levels [*Sarma et al.*, 2000; V. V. S. S. Sarma et al., Carbon budget in the eastern and central Arabian Sea: An Indian JGOFS Synthesis, submitted to *Global Biogeochemical Cycles*, 2003]. SW coast of India contained high pCO_2 levels (~400 μatm) during fall monsoon and the same has been lowered by >40 μatm in the NE monsoon. Weak north-south and east-west variability exists (<10 μatm) in surface pCO_2 levels during this season (Figure 6d).

[23] In summary, surface pCO_2 levels are higher than atmospheric value round the year. The gradient is very large during SW monsoon because of strong physical forcing, whereas it is relatively small during intermonsoons.

5.3. Atmospheric pCO_2

[24] *Goyet et al.* [1998a] have measured atmospheric pCO_2 levels (pCO_2^{air}) during different seasons in the Arabian Sea in 1995. The seasonal amplitude in pCO_2^{air} is 15 μatm with lower pCO_2^{air} in the SW monsoon than in the NE monsoon. This variation was attributed to different source of air masses [*Goyet et al.*, 1998a]. During NE monsoon, wind blows from the northeast over the Indian Peninsula, as a result, the air mass over the Arabian Sea is dominated by a dry continental tropical air mass. On the contrary, during SW monsoon, the air blow from the southwest of the Arabian Sea; hence the air mass above the Arabian Sea is dominated by a moist air from the Indian Ocean.

[25] The levels of pCO_2^{air} decreased from ~355 to 340 μatm from March to July/August, whereas it increased from 340 to 355 μatm during December. Hence I have considered here the minima and maxima in pCO_2^{air} observed during different months by *Goyet et al.* [1998a] over the Arabian Sea, which is assumed to be constant over space. The average monthly variability in pCO_2^{air} is given in Table 3.

5.4. Fluxes of Carbon Dioxide at Air-Sea Interface

[26] The monthly pCO_2 levels are used to estimate air-sea fluxes of CO_2 in the Arabian Sea. The CO_2 fluxes (mmol m^{-2} day^{-1}) can be computed from

$$FCO_2 = Ks\left[pCO_2^{water} - pCO_2^{air}\right] = Ks\Delta pCO_2 \qquad (6)$$

According to *Wanninkhof* [1992] (hereinafter referred to as W-92), the transfer velocity K can be computed from

$$K = 0.39\ u^2[Sc/660]^{-0.5} \qquad (7)$$

Where K is the gas transfer velocity (cm h^{-1}), u is the wind speed (m s^{-1}), s is the CO_2 solubility in seawater [*Weiss*, 1974] and Sc is the Kinematic viscosity of water divided by the diffusion coefficient for CO_2 (i.e., Schmidt number).

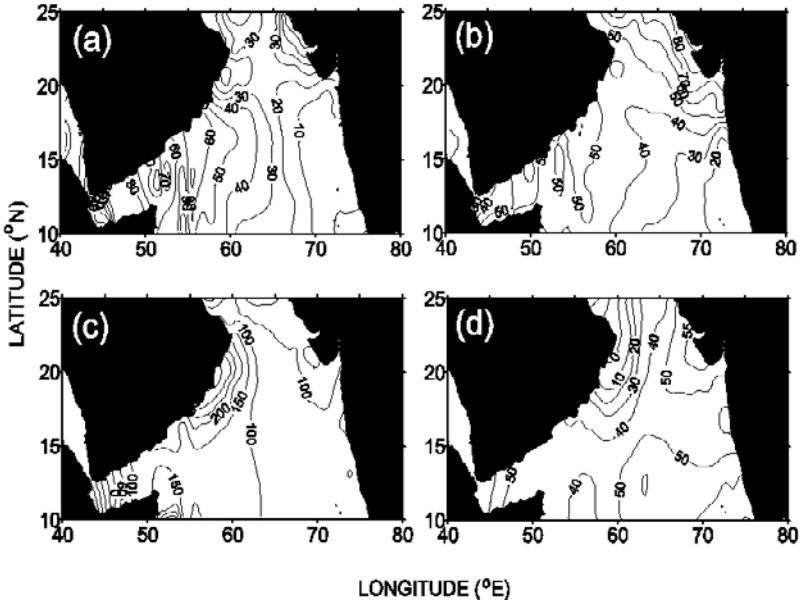

Figure 7. Seasonal and spatial variability in distribution of ΔpCO_2 in the Arabian Sea: (a) NE monsoon, (b) spring intermonsoon, (c) SW monsoon, and (d) fall intermonsoon. Note the contour interval for Figure 7c is 50 μatm.

[27] Recently *Wanninkhof and McGillis* [1999] (hereinafter referred to as WM-99) have found cubic relationship between air-sea exchange of CO_2 and wind speed during Gas Ex-98 in the Atlantic Ocean. On the basis of the field and laboratory studies, they hypothesize that the stronger dependence at high wind speeds is driven by bubble entrainment whereas retardation by surfactants result in weaker dependence at lower winds. They developed a relationship for long term averaged winds assuming a Weibull distribution for average wind speeds from 0–20 m s^{-1} and can be computed long-term gas transfer using the following formulation

$$k = \left[1.09\ u - 0.333\ u^2 + 0.078\ u^3\right](Sc/660)^{0.5} \qquad (8)$$

The transfer velocity computed on the basis of this equation would differ by 25% compared to W-92 at 15 m s^{-1} and it is more at higher wind speeds.

[28] Since most of the earlier budget estimations in the Arabian Sea were done using W-92 formulations, in order to compare my results with previous estimations, I evaluated CO_2 fluxes on the basis of transfer velocity of CO_2 using both W-92 and WM-99. In the equation 6, pCO_2^{water} is the monthly average value of each grid point. The atmospheric pCO_2 value (pCO_2^{air}) is taken from *Goyet et al.* [1998a]. The wind speed data were obtained from *Hellerman and Rosenstein* [1983]. The flux is determined from the product of monthly mean ΔpCO_2 (μatm), monthly mean transfer velocities and Schmidt numbers for each grid point.

5.4.1. ΔpCO_2 Variability

[29] Seasonal averaged ΔpCO_2 distribution has been plotted in Figures 7a–7d. The ΔpCO_2 showed clear north-south as well east west gradients in the Arabian Sea. During all the seasons, higher ΔpCO_2 levels found in the western Arabian Sea (WAS) compared to the east. The N-S variability in ΔpCO_2 is quite prominent during spring and fall intermonsoons and SW monsoon with higher levels in the north (north of 18°N) compared to south. Surface waters are found to be undersaturated with respect to atmospheric pCO_2 along the SW coast of India during NE monsoon. The ΔpCO_2 levels in this region have been increased by 20 μatm during spring intermonsoon. The ΔpCO_2 levels in the northern and western Arabian Sea increased from NE monsoon to SW monsoon and decreased slowly during fall monsoon. The highest ΔpCO_2 of 150–300 μatm has been observed during July–August along the west coast of the Arabian Sea because of intense upwelling. ΔpCO_2 is about 70–80 μatm in the western side of the open ocean because of advection of upwelled waters from the coast. ΔpCO_2 levels in the western Arabian Sea decreased slowly to ~40 μatm during fall intermonsoon.

5.4.2. Wind Speeds and CO_2 Transfer Velocities

[30] Wind speeds showed strong seasonal cycle with higher values during monsoons. The wind speeds range from 5–7 m s^{-1} during January–February while it is 3–5 m s^{-1} from March to April. Wind speeds increased from May to September and with the highest value during July–August (6–18 m s^{-1}). They were 4–6 m s^{-1} in the postmonsoon. In general wind speeds are comparatively higher in the western than eastern Arabian Sea.

[31] The monthly variability in transfer velocity of CO_2 (kCO_2) is computed using the W-92 and WM-99 are given in Figures 8a–8c. The amplitude of kCO_2 variations in the annual cycle is varied from 5–75 cm h^{-1} with maximum in June during SW monsoon (~75 cm h^{-1}) (Figure 8c). Comparatively high kCO_2 values are found during SW monsoon at all regions in the Arabian Sea. In all regions the minima occur during spring and fall monsoon seasons (<10 cm h^{-1}) because of weak winds in these seasons. The kCO_2 computed on the basis of WM-99 are significantly higher than W-92 especially during monsoon when winds are much stronger. As WM-99 showed in their Figure 3,

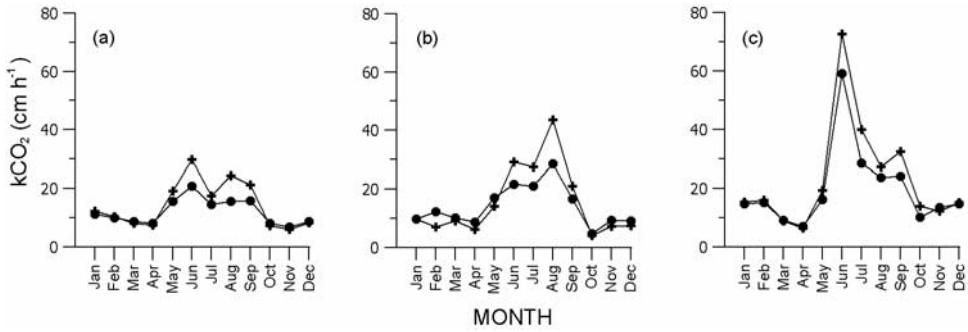

Figure 8. Regional and monthly variability in transfer velocity of carbon dioxide (kCO_2) in the Arabian Sea: (a) WAS, (b) EAS, and (c) NAS.

kCO_2 deviates significantly from the W-92 at the wind speeds >8 m s^{-1}. Nevertheless, these results suggest that air-sea flux of CO_2 is mostly influenced by winds in the open sea regions whereas strong ΔpCO_2 levels would enhances fluxes in the coastal regions.

5.4.3. Monthly Variability in Air-Sea Fluxes of CO_2

[32] Air-sea fluxes of CO_2 indicate that the Arabian Sea is a source of CO_2 to the atmosphere throughout the year, which is in agreement with the earlier reports [*Goyet et al.*, 1998a; *Sarma et al.*, 1998]. The seasonal and spatial variability in CO_2 fluxes computed on the basis of WM-99 in different regions are depicted in Figures 9a–9c. The higher fluxes to the atmosphere were found to occur from June to August in all regions. The Arabian Sea emits 2 to 12 mmol CO_2 m^{-2} d^{-1} to the atmosphere during NE monsoon. Small patch of sink for atmospheric CO_2 is found at the SW coast of India because of Bay of Bengal low-saline water mass (Figure 9a). Comparatively higher fluxes have been noticed during spring than NE monsoon because of high wind speeds. Though, no strong mixing occur during this period, however, the Arabian Sea emits 2 to 4 mmol CO_2 m^{-2} d^{-1} to the atmosphere (Figure 9b). The northeastern Arabian Sea is observed to release more fluxes to the atmosphere (8–10 mmol CO_2 m^{-2} d^{-1}) during spring intermonsoon because of increases in pCO_2 levels (Figure 6b) by intense regeneration of organic matter produced during NE monsoon. The highest fluxes of 20 to 90 mmol CO_2 m^{-2} d^{-1} (Figure 9c) have been observed during SW monsoon. It is due to high ΔpCO_2 driven by coastal as well as Open Ocean upwelling and associated with high winds. This results in emission of higher amounts of CO_2 to the atmosphere. The coastal regions are especially emitting higher quantities of CO_2 to the atmosphere than open ocean region (Figure 9c). As a result of advection of high-pCO_2 upwelled waters in to open ocean, ΔpCO_2 is higher in the open ocean in the northern Arabian Sea leading to high fluxes in the open ocean region as well (>10 mmol CO_2 m^{-2} d^{-1}). Fall monsoon showed low fluxes, like spring intermonsoon, which ranged from 2 to 4 mmol CO_2 m^{-2} d^{-1}. The sea-to-air fluxes computed using W-92 transfer velocity is presented in Table 3. In summary, air-sea fluxes of CO_2 showed strong seasonal and spatial variability because of the existence of different physical associated biogeochemical provinces. In order to understand effect of

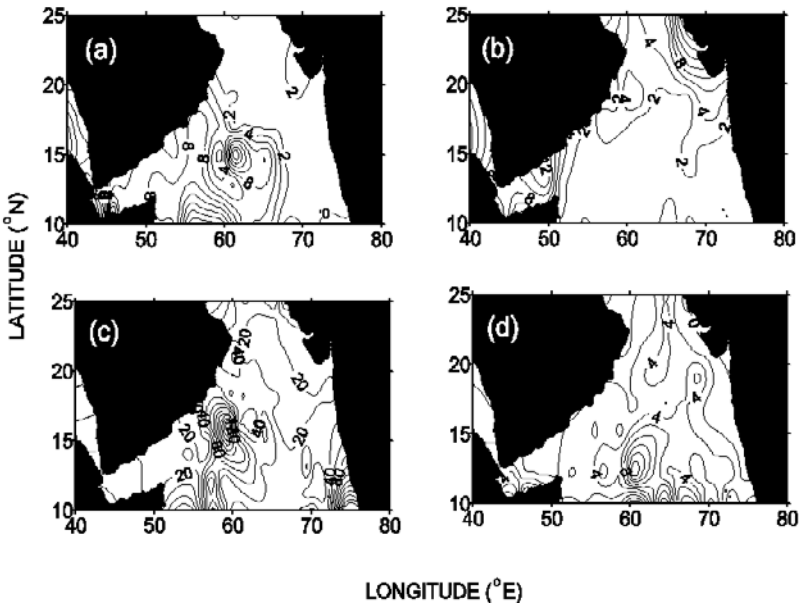

Figure 9. Monthly and spatial distribution of air-sea fluxes of CO_2 in the Arabian Sea: (a) December–February, (b) March–May, (c) June–August, and (d) September–November.

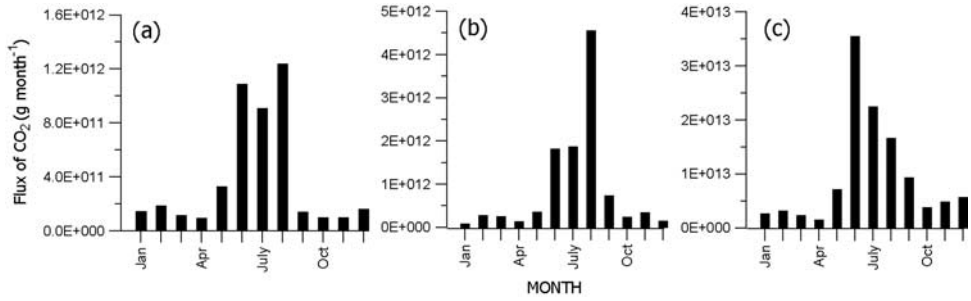

Figure 10. Monthly averaged fluxes of CO_2 for different regions in the Arabian Sea: (a) WAS, (b) EAS, and (c) NAS.

these processes on air-sea exchange of CO_2, regional fluxes and budgets were studied (see Figure 1).

[33] The monthly averaged fluxes of CO_2 based on WM-99 in different regions have been depicted in Figure 10. WAS is a strong source of CO_2 to the atmosphere throughout the year compared to EAS in terms of unit area. The source strength decreases from January to April (Figure 10a). However, the magnitude of decrease in fluxes is quite small because of low ΔpCO_2 during March–May. The source strength increases four folds during May–August (0.3 to 1.24 TgC month^{-1}). September–November it decreased again from 0.14 to 0.1 TgC month^{-1} followed by an increase in December (0.16 TgC month^{-1}).

[34] In contrast to WAS, fluxes have increased from January to May followed by maxima in February in the EAS. This region appears to be a strong source of CO_2 (1.8–4.5 TgC month^{-1}) from June to August. Fluxes decreased from September to December from 0.7 to 0.15 TgC month^{-1}, and unlike in WAS, no increase is found during December as the effect of NE monsoon is comparatively less in the EAS.

[35] Northern Arabian Sea (NAS) showed the pattern similar to WAS. The highest fluxes were observed during June–August with maximal values in June (35.5 TgC month^{-1}) and it increased from October to December (Figure 10c). Though, air-sea pCO_2 gradients are comparatively high, wind speeds are low that result in low fluxes during January–March (2–3 TgC month^{-1}) and November–December (~5 TgC month^{-1}). The minima in fluxes observed during April–May and October can be attributed to low ΔpCO_2 associated with low wind speeds.

[36] It is difficult to estimate all the errors associated with these calculations; an attempt, however, has been made here. The standard error for each of the water pCO_2 values was determined from the quality of the regression line for DIC and TA and through computations of pCO_2 (18–23 μatm). The errors involved in atmospheric pCO_2 measurements are ±2 μatm [*Goyet et al.*, 1998a] and the solubility number is good to about 0.3% [*Weiss*, 1974]. The transfer velocity is a function of wind speed, which has an estimated error of about 2 m s^{-1} and the transfer coefficient, which was estimated by W-92 to have an error of approximately 25%. If all these errors considered in the computation of net fluxes amounts to 2.0×10^{12} mole of carbon. This results to an error of about 30% in the budget computations for the Arabian Sea.

5.4.4. Seasonal Fluxes and Budgets

[37] The area, the seasonal and annual budgets of all regions computed on the basis of W-92 and WM-99 transfer velocities have been presented in Table 4. However, I discussed here the fluxes computed on the basis of WM-99 formulations. WAS showed the highest fluxes compared to rest of the regions in terms of unit area. Comparatively the highest fluxes were observed during SW monsoon. The fluxes were nearly equal magnitude (0.49 to 0.55 TgC season^{-1}; season = 91.25 days) between NE and spring

Table 4. Average Air-Sea Fluxes of Carbon Dioxide and Seasonal and Regional Budget of Fluxes in the Arabian Sea

Region	Area, 10^{12} m^2	Season	pCO_2,[a] μatm	Average Flux,[a] mmol m^{-2} d^{-1} (WM-99)	Budget, 10^{12} Tg yr^{-1}	Average Flux,[a] mmol m^{-2} d^{-1} (W-92)	Budget, 10^{12} g yr^{-1}
WAS	0.10	NE monsoon	415	4.5	0.49	4.3	0.47
		spring monsoon	412	5.0	0.55	4.7	0.51
		SW monsoon	565	38.2	4.18	22.0	2.41
		fall monsoon	378	3.4	0.37	3.1	0.34
		annual			5.59		3.73
EAS	0.27	NE monsoon	391	2.2	0.65	2.2	0.65
		spring monsoon	388	2.5	0.74	1.8	0.53
		SW monsoon	468	18.5	5.58	12.9	3.82
		fall monsoon	408	4.2	1.24	3.9	1.15
		annual			8.21		6.16
NAS	2.15	NE monsoon	397	2.9	6.82	2.8	6.60
		spring monsoon	402	3.2	7.53	3.0	7.08
		SW monsoon	467	22.3	52.5	15.5	36.57
		fall monsoon	402	4.0	9.41	4.2	9.91
		annual			76.26	6.4	60.16

[a]Average value of reconstructed pCO_2/flux for each region and season.

monsoons whereas fall monsoon showed comparatively lower fluxes (0.37 TgC season^{-1}) than that of spring intermonsoon. Annual emission of CO_2 to the atmosphere from the WAS amounts to 5.59 TgC yr^{-1}. East coast of the Arabian Sea (EAS) has the least flux compared to rest of the regions in terms of unit area. Fluxes are ranged between 0.65 to 5.6 TgC season^{-1} with higher fluxes during SW monsoon. On an annual basis, EAS releases 8.21 TgC yr^{-1} to the atmosphere. Northern Arabian Sea (NAS) is the second highest source to the atmosphere in terms of unit area. The highest flux (52.5 TgC season^{-1}) to the atmosphere is observed during SW monsoon. Over all, NAS emits 76.26 TgC yr^{-1} to the atmosphere (Table 4).

[38] On the whole, the Arabian Sea north of 10° N (2.52×10^{12} m^2) releases ~90 TgC to the atmosphere annually for the year 1995 on the basis of WM-99 where as it is smaller (~70 Tg C yr^{-1}) using W-92 transfer velocities respectively. These estimates are in good agreement with other independent estimates of sea-to-air fluxes of CO_2 from the Arabian Sea. For instance, *Takahashi et al.* [2002] have given World Ocean air-sea fluxes of CO_2 maps based on the observed fluxes and interpolations which show Arabian Sea releases ~1–2.5 mole CO_2 m^{-2} yr^{-1} is being released to the atmosphere for the year 1995 and found close to zero fluxes in a small region in the southeast coast of the Arabian Sea, which is consistent with present study. Extrapolation of these fluxes to the study region amounts to efflux of CO_2 to be 30–75.6 TgC yr^{-1} to the atmosphere. This estimate was made on the basis of W-92 transfer velocities, which is consistent with the present budget estimate based on W-92 of 70 TgC yr^{-1}. Recently, *Sabine et al.* [2000] reported that >2 mole CO_2 m^{-2} yr^{-1} is being released to the atmosphere by the Arabian Sea that amounts to >60.5 TgC yr^{-1} for the year 1995 using W-92. In addition to this, *Bhushan et al.* [2000] have estimated air-sea fluxes of CO_2 on the basis of ^{14}C measurements in the Arabian Sea to be 0.7 to 2.4 moles m^{-2} y^{-1}. On the basis of their estimate, the out gassing of CO_2 from the study region amounts to 21–72.5 TgC yr^{-1}. All these independent estimates are in good agreement with the present budget of 70 TgC yr^{-1} based on W-92. However, present model flux estimates is much higher than the *Goyet et al.* [1998a] estimate of 7 Tg yr^{-1} because of the underestimation of surface pCO_2 as large scatter found in the SST to pCO_2 relation. The present study suggest that considering the bubble entrainment influence on transfer velocity of CO_2 would enhance CO_2 fluxes to the atmosphere by ~20% from the study region.

6. Conclusions

[39] This study indicates that the Arabian Sea is a perennial source of CO_2 to the atmosphere. Distribution of surface pCO_2 and fluxes showed large seasonal and spatial variability in the Arabian Sea and are mostly caused by physical associated biological processes. Low-pCO_2 waters were noticed along SW coast of India during NE monsoon because of the entry of Bay of Bengal low-salinity water mass. The surface pCO_2 distribution showed strong north-south gradient during all months with higher values in the north. This resulted from strong physical forcing in the north compared to that in the southern Arabian Sea. The strong east-west gradient is seen especially during SW monsoon because of variable intensities in upwelling in the west and east coasts of the Arabian Sea. The air-sea fluxes of CO_2 showed maxima values from all regions during SW monsoon. Western Arabian Sea seems to release higher CO_2 fluxes to the atmosphere in terms of unit area compared to eastern and northern Arabian Sea. Air-sea fluxes of CO_2 amount to release of 5.6 and 8.2 TgC annually to the atmosphere by west and east coasts while 76.2 TgC is released by northern Arabian Sea respectively. Annual emission of CO_2 from the Arabian Sea is estimated to be 90 TgC yr^{-1} on the basis of WM-99 transfer coefficients which is 20% higher than W-92 (70TgC yr^{-1}).

[40] **Acknowledgments.** This study would not have been possible without considerably efforts of the scientist during U.S. JGOFS, Indian JGOFS study collecting the data. I thank all the carbon group personnel for making available their high-quality data set for processing this model. I would like to thank two anonymous reviewers for their constructive comments for substantial improvement of this manuscript.

References

Barber, R. T., J. Marra, R. C. Bidigare, L. A. Codispoti, D. Halpern, Z. Johnson, M. Latasa, R. Goericke, and S. L. Smith, Primary productivity and its regulation in the Arabian Sea during 1995, *Deep Sea Res., Part II*, *48*, 1127–1172, 2001.

Bhattathiri, P. M. A., A. Pant, S. Sawant, M. Gauns, S. G. P. Matondkar, and R. Mohanraju, Phytoplankton production and chlorophyll distribution in the eastern and central Arabian Sea in 1994–1995, *Curr. Sci.*, *71*, 857–862, 1996.

Bhushan, R., B. L. K. Somayajulu, S. Chakraborty, and S. Krishnaswami, Radiocarbon in the Arabian Sea water column: Temporal variations in bomb ^{14}C inventory since the GEOSECS and CO_2 air-sea exchange rates, *J. Geophys. Res.*, *105*, 14,273–14,282, 2000.

Conkright, M., S. Levitus, T. O'Brien, T. Boyer, J. Antonov, and C. Stephens, World Ocean Atlas 1998 CD-ROM Data Set Documentation, *Tech. Rep. 15*, 16 pp., Natl. Oceanogr. Data Cent., Silver Spring, Md., 1988.

de Sousa, S. N., M. D. Kumar, S. Sardessai, V. V. S. S. Sarma, and P. V. Shirodkar, Seasonal variability in oxygen and nutrients in the central and eastern Arabian Sea, *Curr. Sci.*, *71*, 847–851, 1996.

Dickson, A. G., and F. J. Millero, A comparison of the equilibrium constants for the association of carbonic acid in seawater media, *Deep Sea Res., Part A*, *34*, 1733–1743, 1987.

Findlater, J., A major low-level air current near the Indian Ocean during the northern summer, *Q. J. R. Meterol. Soc.*, *95*, 362–380, 1969.

Findlater, J., The low-level cross-equatorial barrier between the Indian and Pacific Oceans and a likely cause for Wallace's line, *UNESCO Tech. Pap. Mar. Sci.*, *49*, 84–97, 1974.

Goyet, C., and A. Poisson, New determination of carbonic acid dissociation constants in seawater as a function of temperature and salinity, *Deep Sea Res., Part A*, *36*, 1635–1654, 1989.

Goyet, C., F. J. Millero, D. W. O'Sullivan, G. Eischeid, S. J. McCue, and R. G. J. Bellerby, Temporal variations of pCO_2 in surface seawater of the Arabian Sea in 1995, *Deep Sea Res., Part I*, *45*, 609–624, 1998a.

Goyet, G., N. Metzl, F. J. Millero, G. Eischeid, D. O'Sullivan, and A. Poisson, Temporal variation of the sea surface CO_2/carbonate properties in the Arabian Sea, *Mar. Chem.*, *63*, 69–79, 1998b.

Goyet, C., C. Coatanoan, G. Eischeid, T. Amaoka, K. Okuda, R. Healy, and S. Tsunogai, Spatial variations of total CO_2 and alkalinity in the northern Indian Ocean: A novel approach for the quantification of anthropogenic CO2 in seawater, *J. Mar. Res.*, *57*, 137–163, 1999.

Hellerman, S., and M. Rosenstein, Normal monthly wind stress over the world ocean with error estimates, *J. Phys. Oceanogr.*, *13*, 1093–1104, 1983.

Johnson, K. M., A. Körtzinger, L. Mintrop, J. C. Duinker, and D. W. R. Wallace, Coulometric total carbon dioxide analysis for marine studies: Measurement and internal consistency of underway DIC concentrations, *Mar. Chem.*, *67*, 123–144, 1999.

Körtzinger, A., J. C. Duinker, and L. Mintrop, Strong CO_2 emissions from the Arabian Sea during South-West Monsoon, *Geophys. Res. Lett.*, *24*, 1763–1766, 1997.

Kumar, M. D., S. W. A. Naqvi, M. D. George, and D. A. Jayakumar, A sink for atmospheric carbon dioxide in the northeast Indian Ocean, *J. Geophys. Res.*, *101*, 18,121–18,125, 1996.

Lee, K., R. Wanninkhof, R. A. Feely, F. J. Millero, and T. H. Peng, Global relationships of total inorganic carbon with temperature and nitrate in surface seawater, *Global Biogeochem. Cycles*, *14*, 979–994, 2000.

Levitus, S., and T. P. Boyer, *World Ocean Atlas 1994*, vol. 4, *Temperature*, *NOAA Atlas NESDIS*, vol. 4, 129 pp., Natl. Oceanic and Atmos. Admin., Silver Spring, Md., 1994.

Levitus, S., R. Burgett, and T. P. Bayer, *World Ocean Atlas 1994,* vol. 3, *Salinity*, *NOAA Atlas NESDIS*, vol. 3, 111 pp., Natl. Oceanic and Atmos. Admin., Silver Spring, Md., 1994.

Lewis, E., and D. W. R. Wallace, Program developed for CO_2 system calculations, *Rep. ORNL/CDIAC-105*, Carbon Dioxide Inf. Anal. Cent., Oak Ridge Natl. Lab., U.S. Dep. of Energy, Oak Ridge, Tenn., 1998.

Louanchi, F., N. Metzl, and A. Poisson, A modeling the monthly sea surface fCO_2 fields in the Indian Ocean, *Mar. Chem.*, *55*, 265–280, 1996.

Madhupratap, M., S. P. Kumar, P. M. A. Bhattathiri, M. D. Kumar, S. Raghukumar, K. K. C. Nair, and N. Ramaiah, Mechanism of the biological response to winter cooling in the northeastern Arabian Sea, *Nature*, *384*, 549–552, 1996.

Manghnani, V., J. M. Morrison, T. S. Hopkins, and E. Bohm, Advection of upwelled waters in the form of plumes off Oman during the Southwest Monsoon, *Deep Sea Res., Part II*, *45*, 2027–2052, 1998.

Mehrbach, C., C. H. Culberson, J. E. Hawley, and R. M. Pytkowicz, Measurement of the apparent dissociation constants of carbonic acid in seawater at atmospheric pressure, *Limnol. Oceanogr.*, *18*, 897–907, 1973.

Millero, F. J., E. A. Degler, D. W. O'Sullivan, C. Goyet, and G. Eischeid, The carbon dioxide system in the Arabian Sea, *Deep Sea Res., Part II*, *45*, 2225–2252, 1998.

Morrison, J. M., L. A. Codispoti, S. Gaurin, B. Jones, V. Manghnani, and Z. Zheng, Seasonal variation of hydrographic and nutrient fields during the US JGOFS Arabian Sea Process Study, *Deep Sea Res., Part II*, *45*, 2053–2101, 1998.

Muralidheeran, P. M., and S. Prasanna Kumar, Arabian Sea upwelling—A comparison between coastal and open ocean regions, *Curr. Sci.*, *71*, 842–846, 1996.

Narvekar, P. V., S. W. A. Naqvi, A. Jayakumar, V. V. S. S. Sarma, and C. M. Nasnolkar, Chemical signatures of upwelling off southwest coast of India, *Eos Trans*, *AGU*, *77*(46), Fall Meet. Suppl., F389, 1996.

Prasanna Kumar, S., and T. G. Prasad, Winter cooling in the northern Arabian Sea, *Curr. Sci.*, *71*, 834–841, 1996.

Ramaiah, N., S. Raghukumar, and M. Gauns, Bacterial abundance and production in the central and eastern Arabian Sea, *Curr. Sci.*, *71*, 878–882, 1996.

Sabine, C. L., R. Wanninkhof, F. M. Key, C. Goyet, and F. J. Millero, Seasonal CO_2 fluxes in the tropical and subtropical Indian Ocean, *Mar. Chem.*, *72*, 33–53, 2000.

Sarma, V. V. S. S., Variability in forms and fluxes of carbon dioxide in the Arabian Sea, Ph.D. thesis, Goa Univ., Goa, India, 1998.

Sarma, V. V. S. S., M. D. Kumar, M. D. George, and A. Rajendran, Seasonal variability in inorganic carbon components in the central and eastern Arabian Sea, *Curr. Sci.*, *71*, 852–856, 1996.

Sarma, V. V. S. S., M. D. Kumar, and M. D. George, The eastern and central Arabian Sea as a perennial source for atmospheric carbon dioxide, *Tellus, Ser. B*, *50*, 179–184, 1998.

Sarma, V. V. S. S., M. D. Kumar, M. Gauns, and M. Madhupratap, Seasonal controls on surface pCO_2 in the central and eastern Arabian Sea, *Proc. Indian Acad. Sci. Earth Planat. Sci.*, *109*, 471–479, 2000.

Shetye, S. R., and S. S. C. Shenoi, Seasonal cycle of surface circulation in the coastal North Indian Ocean, *Proc. Ind. Acad. Sci. Earth Planet. Sci.*, *97*, 53–62, 1988.

Shetye, S. R., A. D. Gouveia, S. S. C. Shenoi, D. Sundar, G. S. Michael, A. M. Almeida, and K. Santanam, Hydrography and circulation off the west coast of India during the Southwest Monsoon 1987, *J. Mar. Res.*, *48*, 359–378, 1990.

Shetye, S. R., A. D. Gouveia, and S. S. C. Shenoi, Does winter cooling lead to the subsurface salinity minimum off Saurashtra, India?, in *Oceanography of the Indian Ocean*, edited by B. N. Desai, pp., 617–625, Oxford Univ. Press, New York, 1992.

Siegenthaler, U., and J. L. Sarmiento, Atmospheric carbon dioxide and the ocean, *Nature*, *365*, 119–125, 1993.

Takahashi, T., H. Olafsson, J. G. Goddard, D. W. Chipman, and S. C. Sutherland, Seasonal variation of CO_2 and nutrients in the high-latitude surface oceans: A comparative study, *Global Biogeochem. Cycles*, *7*, 843–878, 1993.

Takahashi, T., et al., Global sea-air CO_2 flux based on climatological surface ocean pCO_2, and seasonal biological and temperature effects, *Deep Sea Res., Part II*, *49*, 1601–1622, 2002.

Wanninkhof, R., Relationship between wind speed and gas exchange over the ocean, *J. Geophys. Res.*, *97*, 7373–7382, 1992.

Wanninkhof, R., and W. R. McGillis, A cubic relationship between air-sea CO_2 exchange and wind speed, *Geophys Res Lett.*, *26*, 1889–1892, 1999.

Wanninkhof, R., E. Lewis, R. A. Feely, and F. J. Millero, The optimal carbonate dissociation constants for determining surface water pCO_2 from total alkalinity and total inorganic carbon, *Mar. Chem.*, *65*, 291–301, 1999.

Weiss, R. F., Carbon dioxide in water and seawater: The solubility of a non-ideal gas, *Mar. Chem.*, *2*, 23–215, 1974.

Wyrtki, K., Physical oceanography of the Indian Ocean, in *The Biology of the Indian Ocean*, edited by B. Zeitzschel, pp. 18–36, Springer-Verlag, New York, 1973.

V. V. S. S. Sarma, Hydrospheric-Atmospheric Research Center, Nagoya University, Furo-cho, Chikusa-ku, Nagoya 464-8601, Japan. (sarma@ihas.nagoya-u.ac.jp)